

Scattering in quantum wires and junctions of quantum wires with edge states of quantum spin Hall insulators

Abhiram Soori *

School of Physics, University of Hyderabad, C. R. Rao Road, Gachibowli, Hyderabad-500046, India.

An integral part of scattering theory calculations in continuum quantum systems involves identifying appropriate boundary conditions in addition to writing down the correct Hamiltonian. In the simplest problem of scattering in one dimensional lattice, scattering due to an on-site potential and scattering due to an unequal bond (in otherwise translationally invariant lattice) give different results for scattering amplitudes. While the scattering problems in the continuum and the lattice models can be mapped to one another for scattering due to on-site potential, the equivalent continuum model for scattering due to an unequal bond is missing. We introduce a new parameter c in the boundary condition of the continuum model that is equivalent to scattering due to an unequal bond on the lattice. Further, we study a junction between a normal metal quantum wire and a one dimensional edge of quantum spin Hall insulator (QSHI) in continuum using the parameter c . In the case of a junction between a normal metal quantum wire and the edge of QSHI, we identify the boundary condition that permits maximum transmission. Further, we solve the scattering problem between the junction of quantum wire and QSHI using a lattice model and map it to continuum model results. The problem of transport between four channels of spinful normal metal quantum wire and two channels of QSHI edge is not well-defined. We rectify this situation by formulating the scattering problem in terms of a junction of a semi-infinite normal metal quantum wire with an infinite edge of QSHI, gapping out one semi-infinite section of the QSHI edge by a Zeeman field and applying an appropriate boundary condition at the junction. We calculate the scattering amplitudes analytically.

I. INTRODUCTION

Scattering at a point in one dimensional continuum quantum mechanics is a well studied text book problem, where a delta-function barrier back-scatters an electron¹. This phenomenon has been used in modeling point-like back-scatterers and interfaces extensively in both noninteracting²⁻⁶ and interacting systems⁷. The point scatterers at the normal metal superconductor junction⁴ backscatters the electrons, reducing the probability of Andreev reflection. In magnetic tunnel junctions^{5,6}, the interface modeled by delta function potential limits the electron transmission. In interacting one-dimensional systems⁷, repulsive short range interaction makes the point like scatterer relevant in the sense of renormalization group and hence is non-negligible. In this work, we restrict our discussion to non-interacting electrons. While the point scatterers modeled by delta function barrier in the continuum backscatter electrons, on a lattice, a hopping strength on a bond not equal to the other hopping strengths in an otherwise translationally invariant system (termed bond impurity) can also act as a scatterer. The scattering coefficients for an on-site energy and for an unequal hopping strength on a lattice have different forms. The lattice model for the energy band can be mapped to the continuum model near the band bottom. A natural question that arises then is- ‘what do the two types of scatterers in the lattice model map to when the lattice model is mapped to a continuum model?’ We answer this question.

Topological insulators have attracted attention of researchers in the last decade owing to their exotic properties such as dissipationless transport^{8,9}. They are in-

sulting in the bulk and conducting on the surface/edge. The first example of such a phenomenon where insulating two-dimensional bulk accompanied by conducting edge states dates back to quantum Hall effect¹⁰. It was later shown that conducting edge states in a two-dimensional insulating bulk originating from the topology of the bulk band structure does not require a net magnetic field, and instead a staggered magnetic flux through a honeycomb lattice can do the job¹¹. This was followed by a prediction by Kane and Mele that graphene with spin-orbit coupling is a two-dimensional topological insulator¹². But spin-orbit coupling in graphene is too weak for the bulk gap to be observable. In 2006, Bernevig, Hughes and Zhang theoretically predicted that certain HgTe-CdTe quantum wells are two-dimensional topological insulators¹³. Two-dimensional topological insulators also known as quantum spin Hall insulators (QSHIs) are band insulators that have conducting one dimensional edge states which come in pairs. Soon after, in 2007 it was experimentally shown that in HgTe-CdTe quantum wells, QSHI can be realized¹⁴. After a decade, a two-dimensional material WTe₂ has also been shown to be a QSHI^{15,16}.

Junctions of topological insulators with normal metals are important, since such junctions are basic building blocks of electronic circuits involving topological elements. Junctions between two-dimensional surface states of three-dimensional topological insulators with two-dimensional ferromagnets¹⁷ and two-dimensional superconductors¹⁸ have been studied using a boundary condition which involves a new parameter c . Recently, this boundary condition has been used in: explanation of planar Hall effect in topological insulators¹⁹ and a proposal to identify Majorana bound states²⁰. However, the de-

pendence of scattering amplitudes on c and the optimal value of c which allows maximum current across the junction is not known. The same boundary condition applies to a junction of one-dimensional normal metal with edge states of QSHI. In this work, we study the conductance across such a junction as a function of this parameter and find the optimal value of the parameter c for which the transmission is maximum. Further, we solve the scattering problem at a junction between a quantum wire and a QSHI using a lattice model and map the results to continuum model calculations. The problem of junction between two materials, each being semi-infinite, is common. But such a problem with one material being a spinful normal metal and the other - an edge state of QSHI is ill defined. In this work, we rectify this problem and construct such a junction.

II. SCATTERING IN A NORMAL METAL QUANTUM WIRE

A point scatterer in continuum theory can be modeled either at the level of Hamiltonian, where the Hamiltonian has a Dirac delta function in real space, or by a boundary condition in the wavefunction at the location of the barrier. Though these two approaches are equivalent, we shall follow the latter approach since it can be more easily generalized. The Hamiltonian H , the wavefunction $\psi(x)$ and the boundary conditions can be written down for a metallic system in the following way:

$$H = \left(\frac{\hat{p}^2}{2m} - \mu \right),$$

$$\psi(0^-) = \psi(0^+), \quad \partial_x \psi|_{0^-}^{0^+} = q_0 \psi(0), \quad (1)$$

where μ is the chemical potential which dictates the electron filling of the quantum wire, \hat{p} is the momentum operator and q_0 quantifies the strength of the impurity which backscatters the electron. The wavefunction for an electron incident from left to right at an energy E takes the form:

$$\psi(x) = e^{ikx} + r_k e^{-ikx} \quad \text{for } x < 0$$

$$= t_k e^{ikx} \quad \text{for } x \geq 0, \quad (2)$$

where $k = \sqrt{2m(\mu + E)}/\hbar$. By matching the boundary conditions, it can be shown that

$$t_k = 2ik/(2ik - q_0) \text{ and } r_k = q_0/(2ik - q_0) \quad (3)$$

This problem can be also stated on a one-dimensional lattice system where on-site energy on one site is different from others in an otherwise regular lattice. The formula for scattering amplitudes is similar to eq. (3) near the band bottom, where the dispersion is quadratic. However, there is a different way of inducing backscattering on a regular infinite one dimensional lattice, which is to simply change the hopping element on one of the bonds

in the otherwise translationally invariant lattice. To define the problem more precisely, we resort to the second quantized language on an infinite one dimensional lattice:

$$H = -w \sum_{n \neq 0} [c_{n+1}^\dagger c_n + \text{h.c.}] - w'(c_1^\dagger c_0 + \text{h.c.})$$

$$-(\mu - 2w) \sum_n c_n^\dagger c_n, \quad (4)$$

where the hopping amplitude w' may not be equal to w . The scattering wavefunction for an electron incident from left to right has the form

$$\psi_n = e^{ikan} + r_k e^{-ikan}, \quad \text{for } n \leq 0,$$

$$= t_k e^{ikan} \quad \text{for } n \geq 1, \quad (5)$$

where a is the lattice spacing and $ka = \cos^{-1}[-(\mu - 2w + E)/2w]$. A scattering wavefunction corresponds to an electron extended throughout the system over an infinite number of sites, in contrast to a bound state whose wavefunction is confined to a particular region and decays exponentially away from the region¹. When $w \neq w'$, a generic electron is backscattered. Transmission and reflection amplitudes can be found from Schrödinger equation to be

$$t_k = \frac{-2iw'w \sin ka}{(w^2 e^{-ika} - w'^2 e^{ika})}$$

$$r_k = \frac{(w'^2 - w^2) e^{ika}}{(w^2 e^{-ika} - w'^2 e^{ika})}. \quad (6)$$

In the limit of small filling, the Fermi energy in both lattice and continuum models lies close to the band bottom. Hence, the lattice dispersion can be approximated to a quadratic dispersion, thereby mapping the continuum model to the lattice model. However, the expressions for the scattering amplitudes: eq. (3) and eq. (6) cannot be mapped on to one another for small k . This means that the two kinds of scatterers are inequivalent.

To find the continuum equivalent of the unequal bond that causes backscattering, let us investigate the continuum theory. The boundary conditions given in eq. (1) for the continuum theory come from continuity of the probability current on either sides of the impurity. This means $\text{Im}[\psi^* \partial_x \psi]$ is continuous at $x = 0$. This implies that a more general boundary condition is

$$\psi(0^-) = c\psi(0^+), \quad \text{and}$$

$$\partial_x \psi|_{0^-} - q_0 \psi(0^-) = \frac{1}{c} [\partial_x \psi|_{0^+} - q_0 \psi(0^+)], \quad (7)$$

where c , q_{0-} and q_{0+} are new parameters that take real values. q_{0-} (q_{0+}) physically means the strength of a delta function impurity at the location $x = 0^-$ ($x = 0^+$). Now, solving for the scattering coefficients in the wavefunction given by eq. (2) from the above boundary condition, we get

$$t_k = \frac{2ick}{ik(c^2 + 1) + c^2 q_{0-} - q_{0+}}, \quad \text{and}$$

$$r_k = \frac{ik(c^2 - 1) - c^2 q_{0-} + q_{0+}}{ik(c^2 + 1) + c^2 q_{0-} - q_{0+}}. \quad (8)$$

In the limit of small k , eq. (6) matches with eq. (8) for the choice $c = w'/w$, $q_{0-} = q_{0+} = 1/a$. Thus, we have mapped the problem of unequal bond that causes backscattering to the continuum theory with appropriate boundary conditions. Physically, the new parameter c in the boundary conditions corresponds to the extent to which the hopping parameter at the junction w' is different from the hopping strength w in the quantum wires. For the choice $q_{0-} = q_{0+} = 1/a$, the limit $c = 1$ corresponds to the junction that allows perfect transmission, while a value of c away from 1 corresponds to an imperfect junction that results in backscattering. The boundary condition in eq. (7) does not follow from a continuum Hamiltonian.

III. SCATTERING AT A JUNCTION OF NORMAL METAL QUANTUM WIRE AND SINGLE EDGE OF QSHI

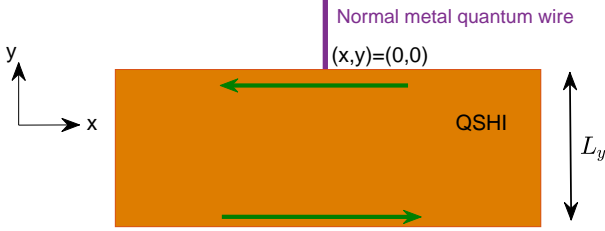


FIG. 1. Schematic diagram of the junction proposed. Normal metal quantum wire (magenta) meets a QSHI. The QSHI is taken to be infinite along x -direction, running from $x = -\infty$ on the left extreme to $x = \infty$ on the right extreme. The coordinate y runs along the vertical direction with value $y = \infty$ on top extreme, a one dimensional quantum wire extends from $y = \infty$ to $y = 0$ (and $x = 0$) to meet the QSHI at $(x, y) = (0, 0)$. Green arrows show the up-spin edge states on the two boundaries of QSHI.

In this section, we study the case of the quantum wire being connected to edge states at only one edge of the QSHI and the edge states on the two ends of the QSHI being decoupled. The Hamiltonian for edge states of QSHI is:

$$H = i\hbar v_F \sigma_z \partial_x, \quad (9)$$

where σ_z is a Pauli spin matrix and v_F is the Fermi velocity. Let us consider a normal metal quantum wire extending from $y = 0$ to $y = \infty$ making a junction with QSHI edge at $x = 0$, $y = 0$. The schematic of the junction being considered can be seen in Fig. 1. The Hamiltonian for normal metal quantum wire is $H_3 = (-\hbar^2 \partial_y^2 / 2m - \mu) \sigma_0$, where m is the effective mass and μ is the chemical potential. We mark the three sides of the junction 1, 2 and 3, where side-1 corresponds to QSHI edge $x < 0$, side-2 corresponds to QSHI edge $x > 0$ and side-3 corresponds to normal metal quantum wire $y > 0$. We denote the

wavefunctions in these three regions by ψ_1 , ψ_2 and ψ_3 respectively. In regions 1 and 2, the spin is locked to the momentum. An up-spin electron with energy E incident from the quantum wire onto the junction has a wavefunction of the form:

$$\begin{aligned} \psi_3(y) &= e^{-ik_3 y} |\uparrow\rangle + r_\uparrow e^{ik_3 y} |\uparrow\rangle + r_\downarrow e^{ik_3 y} |\downarrow\rangle, \\ \psi_1(x) &= t_1 e^{-ik_x x} |\uparrow\rangle, \\ \psi_2(x) &= t_2 e^{ik_x x} |\downarrow\rangle, \end{aligned} \quad (10)$$

where $|\uparrow\rangle = [1, 0]^T$, $|\downarrow\rangle = [0, 1]^T$ are the spinors, $k_3 = \sqrt{2m(\mu + E)}/\hbar$ and $k_x = E/(\hbar v_F)$. The time reversal invariant boundary condition that relates these wavefunctions is given by^{17,18}:

$$\begin{aligned} \psi_3 &= c[M(\chi_1)\psi_1 + M(\chi_2)\psi_2], \\ \frac{\hbar}{mv_F} \partial_y \psi_3 - 2\chi_3 \psi_3 &= -\frac{i}{c} \sigma_z [M(\chi_1)\psi_1 - M(\chi_2)\psi_2], \end{aligned} \quad (11)$$

where $M(\chi) = \cos \chi - i \sin \chi \sigma_z$. This boundary condition conserves current. The parameters χ_i , $i = 1, 2$ physically mean the barrier strengths on sides $i = 1, 2$ of the QSHI edge²¹. Due to Klein tunneling, the barriers χ_1 and χ_2 on the QSHI edge allow perfect transmission and hence they can be set to zero. The calculation in the previous section suggests that the parameter c is physically related to hopping from quantum wire to the QSHI edge. The parameter χ_3 corresponds to the delta function barrier strength close to the junction on the quantum wire. Let us set $\chi_i = 0$ for $i = 1, 2, 3$ and calculate the scattering coefficients in eq. (10) using the boundary condition in eq. (11). This gives us

$$\begin{aligned} r_\downarrow &= t_2 = 0, \\ t_1 &= \frac{2\hbar k_3 c}{mv_F + c^2 \hbar k_3}, \\ r_\uparrow &= \frac{\hbar k_3 c^2 - mv_F}{mv_F + c^2 \hbar k_3}. \end{aligned} \quad (12)$$

It is expected that the scattering coefficients in the spin down channels are zero, since the incident electron is spin up and the full Hamiltonian commutes with σ_z . The transmission amplitude t_1 is a function of c and it can be shown that it is maximum for the choice $c = \pm \sqrt{mv_F / \hbar k_3}$. In fact, c can be a function of energy and here, let us choose $c = \sqrt{mv_F / \hbar k_3}$. For this choice of c , $t_1 = \sqrt{\hbar k_3 / (mv_F)}$. This expression for transmission amplitude can have a value larger than 1. But the differential conductance $G_{13} = dI_1 / dV_3$, the ratio of differential current on side-1 to the differential voltage applied on side-3 is given by

$$G_{13} = \frac{e^2 v_F}{2\pi} \frac{dk_3}{dE} |t_1|^2 = \frac{e^2}{h} \frac{mv_F}{\hbar k_3} \left[\frac{2c \hbar k_3}{mv_F + c^2 \hbar k_3} \right]^2, \quad (13)$$

where the factor of $(1/2\pi)(dk_3/dE)$ is due to the density of states of the incident electrons. It can be easily shown that G_{13} for the special choice of $c = \pm \sqrt{mv_F / (\hbar k_3)}$ will be e^2/h . In Fig. 2 we plot G_{13} versus $c \sqrt{\hbar k_3 / (mv_F)}$.

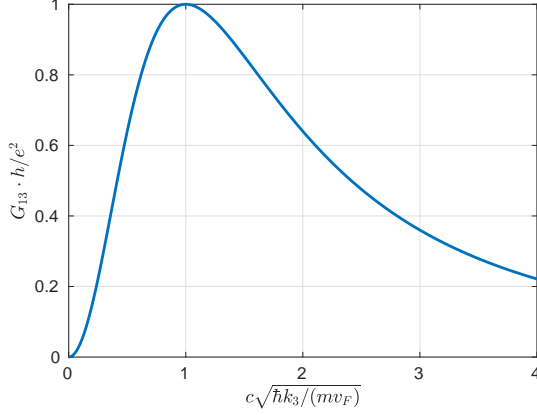


FIG. 2. Conductance G_{13} as a function of $c\sqrt{\hbar k_3}/(mv_F)$ from eq. (13). It can be seen that when $c\sqrt{\hbar k_3}/(mv_F) = 1$, the conductance is maximum and the transmission is perfect at $G_{13} = e^2/h$.

In other words, in an energy window between E and $E + dE$, the incident current on side-3 is:

$$e \frac{dk_3}{2\pi} v = e \frac{dk_3}{2\pi} \frac{dE}{\hbar dk_3} = \frac{e}{h} dE$$

The transmitted current on side-1 is $eD(E)dE|t_1|^2 v_F$ where $D(E) = (1/2\pi)(dk_3/dE)$ is the density of states of incident electrons. This is the same as $(e/2\pi)v_F|t_1|^2 dk_3$ which reduces to $(e/h)dE$ for the special choice of $c = \sqrt{mv_F/\hbar k_3}$. Hence, though t_1 can have a magnitude larger than 1, the incident current is exactly equal to the transmitted current due to the multiplicative factor $D(E)$.

IV. CONDUCTANCE OF JUNCTION OF QUANTUM WIRE WITH QSHI FROM LATTICE MODEL

In this section, we describe transport calculation on a junction of quantum wire with QSHI described by tight

binding model. QSHI is essentially two copies of Chern insulator, with one copy being the time reversed partner of the other²². As we have seen in the previous section, the scattering problem can be solved separately in spin sectors that are eigenstates of σ_z since σ_z commutes with the full Hamiltonian. In this section, we study the scattering problem in the $|\uparrow\rangle$ -spin sector. One main qualitative difference from the previous section is that, here, the width of the QSHI is finite and the edge states from the two boundaries hybridize, opening up the possibility of an up-spin electron incident from the quantum wire getting transmitted either to the left or right on the QSHI. The lattice Hamiltonian for quantum wire can be written as $H_{3L} = \sum_{n=1}^{\infty} [-w(c_{n+1}^\dagger c_n + \text{h.c.}) - \mu_l c_n^\dagger c_n]$, where c_n is the annihilation operator for an electron at site n . The lattice for each spin component of QSHI is a bipartite lattice with two lattice sites per unit cell. Defining $c_{n_x, n_y} = [c_{n_x, n_y, 1}, c_{n_x, n_y, 2}]^T$, where $c_{n_x, n_y, j}$ is annihilation operator at site (n_x, n_y) with sublattice j , the Hamiltonian for QSHI can be written as

$$\begin{aligned} H_Q = & \sum_{n_x=-\infty}^{\infty} \sum_{n_y=-L_y+1}^0 \left[(\Delta - 4B) c_{n_x, n_y}^\dagger \tau_z c_{n_x, n_y} \right. \\ & + c_{n_x+1, n_y}^\dagger (B\tau_z + \frac{iA}{2}\tau_x) c_{n_x, n_y} \\ & \left. + c_{n_x-1, n_y}^\dagger (B\tau_z - \frac{iA}{2}\tau_x) c_{n_x, n_y} \right] + \sum_{n_x=-\infty}^{\infty} \sum_{n_y=-L_y+1}^{-1} \\ & \left[c_{n_x, n_y+1}^\dagger (B\tau_z + \frac{iA}{2}\tau_y) c_{n_x, n_y} + \text{h.c.} \right], \end{aligned} \quad (14)$$

where τ_i ($i = x, y, z$) are the Pauli spin matrices acting on the sublattice space. QSHI is in topological phase hosting edge states when $0 < \Delta < 8B$. The full Hamiltonian for the junction of quantum wire connected to a QSHI is $H = H_Q + H_{3L} + H_{WQ}$, where $H_{WQ} = -w_{nq}(c_1^\dagger c_{0,0,1} + \text{h.c.})$ and w_{nq} is the hopping strength that connects the normal metal quantum wire to the QSHI.

Using the above Hamiltonian H in Schrödinger wave equation, the eigenstate

$$|\psi\rangle = \sum_{n=1}^{\infty} \psi_{3,n}^w |3, n\rangle + \sum_{n_x=-\infty}^{\infty} \sum_{n_y=-L_y+1}^0 \sum_{i=1,2} \psi_{n_x, n_y, i} |n_x, n_y, i\rangle \quad (15)$$

(where $\psi_{3,n}^w$ is the wavefunction on the quantum wire and $\psi_{n_x, n_y, i}$ is wavefunction on the QSHI site) can be shown to obey the equations

$$\begin{aligned} E\psi_{3,1}^w &= -\mu_l \psi_{3,1}^w - w\psi_{3,2}^w - w_{nq}\psi_{0,0,1}, \\ E\psi_{0,0} &= -w_{nq} \begin{bmatrix} \psi_{3,1}^w \\ 0 \end{bmatrix} + (B\tau_z + \frac{iA}{2}\tau_y)\psi_{0,-1} + (\Delta - 4B)\tau_z\psi_{0,0} + (B\tau_z + \frac{iA}{2}\tau_x)\psi_{-1,0} + (B\tau_z - \frac{iA}{2}\tau_x)\psi_{1,0}, \end{aligned}$$

$$\begin{aligned}
E\psi_{n_x, n_y} &= (B\tau_z + \frac{iA}{2}\tau_x)\psi_{n_x-1, n_y} + (\Delta - 4B)\tau_z\psi_{n_x, n_y} + (B\tau_z - \frac{iA}{2}\tau_x)\psi_{n_x+1, n_y} + (B\tau_z + \frac{iA}{2}\tau_y)\psi_{n_x, n_y-1} \\
&\quad + (B\tau_z - \frac{iA}{2}\tau_y)\psi_{n_x, n_y+1}, \text{ for } n_x = -1, 0, 1 \text{ and } -L_y + 2 \leq n_y \leq -1, \\
E\psi_{n_x, -L_y+1} &= (B\tau_z + \frac{iA}{2}\tau_x)\psi_{n_x-1, -L_y+1} + (\Delta - 4B)\tau_z\psi_{n_x, -L_y+1} + (B\tau_z - \frac{iA}{2}\tau_x)\psi_{n_x+1, -L_y+1} \\
&\quad + (B\tau_z - \frac{iA}{2}\tau_y)\psi_{n_x, -L_y+2}, \text{ for } n_x = -1, 0, 1 \\
E\psi_{n_x, 0} &= (B\tau_z + \frac{iA}{2}\tau_x)\psi_{n_x-1, 0} + (\Delta - 4B)\tau_z\psi_{n_x, 0} + (B\tau_z - \frac{iA}{2}\tau_x)\psi_{n_x+1, 0} + (B\tau_z + \frac{iA}{2}\tau_y)\psi_{n_x, -1}, \\
&\quad \text{for } n_x = -1, 1,
\end{aligned} \tag{16}$$

where $\psi_{n_x, n_y} = [\psi_{n_x, n_y, 1}, \psi_{n_x, n_y, 2}]^T$. The dispersion of quantum wire is $E = -2w \cos k_3 - \mu_l$. The QSHI Hamiltonian H_Q is translationally invariant along x and has $2L_y$ bands. For $L_y = 4$, $A = 3\Delta$, and $B = 2\Delta$, the dispersion for H_Q is plotted in Fig. 3. The bands closest to zero energy are the edge state bands.

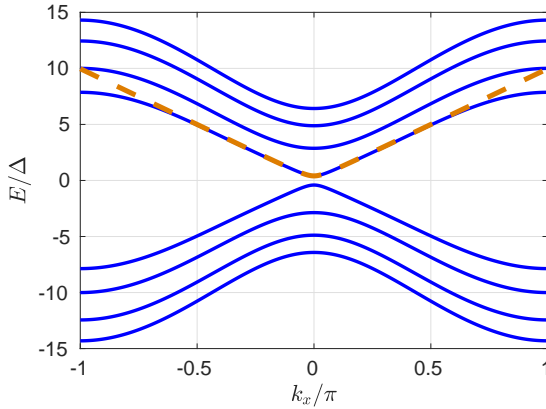


FIG. 3. Dispersion of QSHI lattice for $L_y = 4$, $A = 3\Delta$ and $B = 2\Delta$. Yellow dashed line is a fit to the positive lowest energy band with the form $E = \sqrt{(\hbar v_F k_x)^2 + \gamma^2}$. We get $\gamma = 0.4089\Delta$ and $\hbar v_F = 3.171\Delta$.

The scattering wavefunction for an electron incident from the quantum wire has the form:

$$\begin{aligned}
\psi_{3,n}^w &= e^{-ikn} + r_k e^{ikn}, \text{ for } n \geq 1 \\
\psi_{n_x, n_y} &= \sum_{j=1}^{2L_y} t_{R,j} e^{ik_{x,j} n_x} \chi_{n_y}(k_{x,j}), \text{ for } n_x \geq 1, \\
&= \sum_{j=1}^{2L_y} t_{L,j} e^{-ik_{k,j} n_x} \chi_{n_y}(-k_{k,j}), \text{ for } n_x \leq -1,
\end{aligned} \tag{17}$$

where $\chi_{n_y}(k_x) = [\chi_{2n_y+1}^0(k_x), \chi_{2n_y+2}^0(k_x)]^T$, $\chi^0(k_x) = [\chi_1^0, \chi_2^0, \dots, \chi_{2L_y}^0]^T$ is the eigenspinor of H_Q with momentum $\hbar k_x$. For every $k_{x,j}$, $-k_{x,j}$ is also a solution of the dispersion relation. At a given energy E , $k_{x,j}$ is chosen so that if $k_{x,j}$ is real, $\partial E / \partial k_{x,j} > 0$, and if $k_{x,j}$ is complex, $\text{Im}[k_{x,j}] > 0$. The values of $k_{x,j}$ at a given energy $E > \gamma$ are found numerically. From eq. (16), the scattering coefficients r_k , $t_{L,j}$'s and $t_{R,j}$'s are found numerically for $w = 15\Delta$, $\mu_l = -2w$ and w_{nq} in the range $[0.1, 80]\Delta$. The

currents in the QSHI for $n_x \geq 1$ (side-2) and $n_x \leq 1$ (side-1) are carried by only the k_{x,j_0} which is real and within the bulk gap, there is only one such pair $(k_{x,j_0}, -k_{x,j_0})$. The differential conductance $G_{j,3}$ the ratio of infinitesimal change in current on side- j to infinitesimal change in voltage on side-3 (normal metal quantum wire) when the bias is changed from $E = eV$ to $E + dE = e(V + dV)$ is given by

$$\begin{aligned}
G_{3,3}(E) &= \frac{e^2}{h} |r_k(E)|^2, \\
G_{1,3}(E) &= -\frac{e^2}{h} \frac{|t_{L,j_0}(E)|^2}{2w \sin k_3} \sum_{n_y=0}^{L_y-1} [\chi_{n_y}(-k_{x,j_0})]^\dagger \\
&\quad \cdot [A \cos k_{x,j_0} \tau_x + 2B \sin k_{x,j_0} \tau_z] \chi_{n_y}(-k_{x,j_0}), \\
G_{2,3}(E) &= \frac{e^2}{h} \frac{|t_{R,j_0}(E)|^2}{2w \sin k_3} \sum_{n_y=0}^{L_y-1} [\chi_{n_y}(k_{x,j_0})]^\dagger [A \cos k_{x,j_0} \tau_x \\
&\quad - 2B \sin k_{x,j_0} \tau_z] \chi_{n_y}(k_{x,j_0}).
\end{aligned} \tag{18}$$

The conductances G_{j3} are numerically evaluated using the lattice model and plotted in Fig. 4 for $E = 0.5\Delta$ as functions of the hopping amplitude w_{nq} . In the next section, we shall discuss a continuum model with boundary conditions that can be used to arrive at these results.

V. CONTINUUM MODEL CALCULATIONS FOR A JUNCTION OF QUANTUM WIRE WITH QSHI EDGE STATES

In this section, we propose the boundary conditions that characterize a junction between quantum wire and QSHI edge states. Similar to the discussion in the previous section, we shall focus our attention to $|\uparrow\rangle$ -spin sector. We shall map the lattice problem of the previous section to continuum. The Hamiltonian of quantum wire is $H_3 = -\hbar^2 \partial_y^2 / 2m$, where $m = \hbar^2 / 2w$ and y takes values in the range $(0, \infty)$. The $|\uparrow\rangle$ -spin is left mover on the top edge and right mover on the bottom edge as

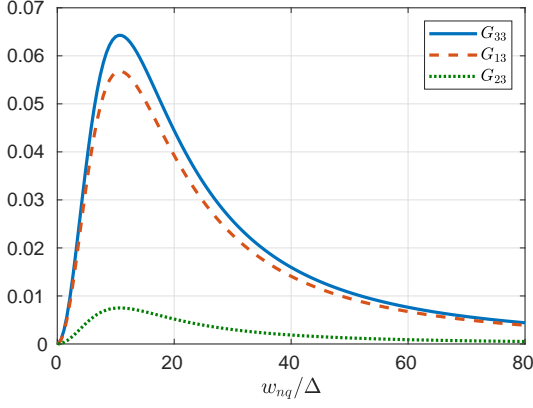


FIG. 4. The conductances G_{33} , G_{13} , G_{23} in units of e^2/h versus w_{nq} for $w = 15\Delta$, $\mu_l = -30\Delta$, $A = 3\Delta$, $B = 2\Delta$ and $E = 0.5\Delta$.

depicted in Fig. 1 and the two modes are coupled. The Hamiltonian for $|\uparrow\rangle$ -spin edge states can be written as $H_Q = i\hbar v_F \eta_z \partial_x + \gamma \eta_x$, where η_x and η_z are Pauli spin matrices whose components correspond to the top and the bottom edge, γ is the coupling strength that couples the two edges and v_F is the Fermi velocity. The dispersion of QSHI edge states from this Hamiltonian is $E = \pm \sqrt{(\hbar v_F k_x)^2 + \gamma^2}$. From the dispersion of QSHI lattice shown in Fig. 3, values of γ and $\hbar v_F$ are found to be $\gamma = 0.4089\Delta$ and $\hbar v_F = 3.171\Delta$ by mapping the continuum dispersion for small k_x .

The current conservation at the junction between quantum wire and QSHI edge can be written as

$$\frac{\hbar^2}{m} \text{Im} \left[\psi_3^\dagger \frac{\partial \psi_3}{\partial y} \right] = \hbar v_F [\psi_2^\dagger \eta_z \psi_2 - \psi_1^\dagger \eta_z \psi_1], \quad (19)$$

all evaluated at $y = 0$ and $x = 0$. The boundary condition which satisfies current conservation is:

$$a \begin{bmatrix} p_1 \psi_3 \\ q_1 \psi_3 \end{bmatrix} = c_1 \psi_1, \quad (20)$$

$$-a \begin{bmatrix} r_1 \partial_y \psi_3 \\ s_1 \partial_y \psi_3 \end{bmatrix} = i \frac{m v_F}{\hbar c_1} \eta_z \psi_1, \quad (21)$$

$$b \begin{bmatrix} p_2 \psi_3 \\ q_2 \psi_3 \end{bmatrix} = c_2 \psi_2, \quad (22)$$

$$b \begin{bmatrix} r_2 \partial_y \psi_3 \\ s_2 \partial_y \psi_3 \end{bmatrix} = i \frac{m v_F}{\hbar c_2} \eta_z \psi_2, \quad (23)$$

where a , b , p_i , q_i , r_i , s_i are real-valued unknowns satisfying $a^2 + b^2 = 1$ and $p_i r_i + q_i s_i = 1$ for $i = 1, 2$, c_1 and c_2 are variables used to define the boundary condition. Here, all the ψ_i 's and the derivatives are evaluated at $y = 0$ or $x = 0$. The scattering wavefunction has the form:

$$\begin{aligned} \psi_3(y) &= e^{-ik_3 y} + r_k e^{ik_3 y}, \\ \psi_1(x) &= t_L e^{-ik_x x} [u_1, v_1], \quad \text{for } x < 0, \\ \psi_2(x) &= t_R e^{ik_x x} [u_2, v_2], \quad \text{for } x > 0, \end{aligned} \quad (24)$$

where $k_3 = \sqrt{2mE}/\hbar$, $k_x = \sqrt{E^2 - \gamma^2}/(\hbar v_F)$, $u_1 = u_2 = \gamma$, $v_1 = E - \hbar v_F k_x$ and $v_2 = E + \hbar v_F k_x$.

Using the wavefunction in eq. (24) in the boundary condition equations (20), (21), (22), and (23), further progress can be made. From eq. (20), it can be seen that $p_1/q_1 = u_1/v_1$ and eq. (21) implies $r_1/s_1 = -u_1/v_1$. Similarly, from eq. (22) and eq. (23), $p_2/q_2 = u_2/v_2$ and $r_2/s_2 = -u_2/v_2$. The unknowns p_i, q_i, r_i, s_i can be parametrized by μ_i, ν_i in the following way: $p_i = \mu_i u_i$, $q_i = \mu_i v_i$, $r_i = -\nu_i u_i$ and $s_i = \nu_i v_i$. The equation $p_i r_i + q_i s_i = 1$ implies $\mu_i \nu_i = 1/(v_i^2 - u_i^2)$. The unknown μ_1 can be set to 1. By finding the expression for r_k from eq. (20) and eq. (21), and equating that expression to the expression for r_k obtained by solving eq. (22) and eq. (23), it can be shown that $\mu_2^2 = -(c_1^2/c_2^2)[(v_1^2 - u_1^2)/(v_2^2 - u_2^2)]$. The parameters a, b describe the fractions of the current from quantum wire that go into the left and the right sides of QSHI and need to be specified. a^2 is the fraction of current incident from quantum wire that goes into side-1 of QSHI and the fraction b^2 goes into side-2. The scattering coefficients r_k, t_L, t_R can be found to be:

$$\begin{aligned} r_k &= \frac{\hbar k c_1^2 - m v_F (u_1^2 - v_1^2)}{\hbar k c_1^2 + m v_F (u_1^2 - v_1^2)} \\ t_L &= -\frac{2 a c_1 \hbar k}{\hbar k c_1^2 + m v_F (u_1^2 - v_1^2)} \\ t_R &= \frac{2 b c_1 \hbar k}{\hbar k c_1^2 + m v_F (u_1^2 - v_1^2)} \sqrt{\frac{u_1^2 - v_1^2}{v_2^2 - u_2^2}} \end{aligned} \quad (25)$$

Here, while c_1 , a and b will depend on w_{nq} , they may also may depend on energy E . The conductances can be found from these scattering coefficients by the formulae:

$$\begin{aligned} G_{33}(E) &= \frac{e^2}{h} (1 - |r_k|^2) \\ G_{13}(E) &= \frac{e^2}{h} \frac{m v_F (u_1^2 - v_1^2)}{\hbar k} |t_L|^2 \\ G_{23}(E) &= \frac{e^2}{h} \frac{m v_F (v_2^2 - u_2^2)}{\hbar k} |t_R|^2. \end{aligned} \quad (26)$$

From the data used to generate Fig. 4, by fitting the lattice model results for G_{33} , r_k can be obtained using eq. (26). From this value of r_k , c_1 can be obtained by fitting with eq. (25). The value of c_1 so obtained is plotted as a function of w_{nq} in Fig. 5. The parameter a can also be fitted by fitting G_{13} and at $E = 0.5\Delta$, $a = 0.9398$ for all values of w_{nq} .

When the two edges of QSHI decouple, $u_1 = 1$ and $v_1 = 0$ and when $a = 1$, the boundary condition in eq. (20)-(23) reduces to the boundary conditions in eq. (11) with $\chi_1 = \chi_2 = \chi_3 = 0$.

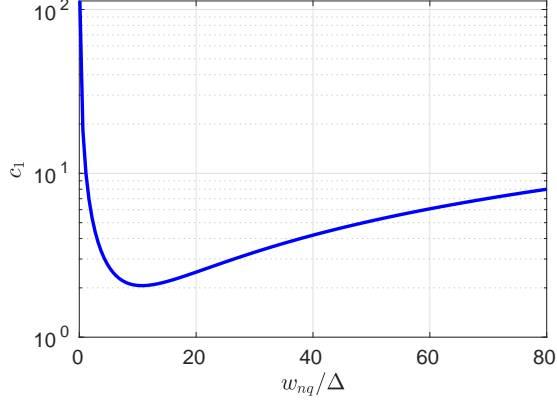


FIG. 5. Value of c_1 obtained by fitting lattice model results of Fig. 4 with continuum model result of eq. (3) versus w_{nq} for $E = 0.5\Delta$.

VI. JUNCTION OF A NORMAL METAL QUANTUM WIRE WITH SEMI-INFINITE QSHI EDGE

The edge states of QSHI live on the boundary of a two-dimensional QSHI. Hence, they cannot be semi-infinite. But a Zeeman field perpendicular to the easy axis of the edge state electrons opens a gap in the spectrum of edge states²³ and this fact can be employed to make the infinitely long edge semi-infinite by applying a Zeeman field to a semi-infinite section of the QSHI edge. We achieve this by a modification of the system in the previous section where the Hamiltonians in regions 1 and 3 remain the same, while the Hamiltonian in region 2 is given by

$$H_2 = i\hbar v_F \sigma_z \partial_x + b \sigma_x. \quad (27)$$

We are interested in the energy range $|E| < b$. Also, we choose $\mu > b$. The wavefunction in the region 2 has the form

$$\psi_2(x) = t_2 e^{\kappa x} |\kappa\rangle, \quad (28)$$

where $\kappa = \sqrt{b^2 - E^2}/\hbar v_F$ and $|\kappa\rangle = [(E + i\hbar v_F \kappa), b]^T$ is the corresponding eigenspinor. We now solve the scattering problem for incident electrons from the quantum wire using the boundary condition in eq. (11) with the choice $\chi_i = 0$ for $i = 1, 2, 3$.

For an up spin electron incident from the quantum wire, the wavefunctions ψ_1 and ψ_3 have the same form as in eq. (10) and the scattering coefficients obtained on solving have the same form as in eq. (12). This is because, an up spin electron incident on the junction from the quantum wire has zero transmission amplitude in region-2 even in the limit of $b = 0$.

For a down spin electron incident from the quantum wire, the wavefunction ψ_1 has the form as in eq. (10) and the wavefunction ψ_2 has the form as in eq. (28). The wave function in region 3 has a form

$$\psi_3(y) = e^{-ik_3 y} |\downarrow\rangle + r_\uparrow e^{ik_3 y} |\uparrow\rangle + r_\downarrow e^{ik_3 y} |\downarrow\rangle, \quad (29)$$

and the scattering amplitudes obtained after solving are

$$\begin{aligned} r_\downarrow &= \frac{\hbar k_3 c^2 - m v_F}{\hbar k_3 c^2 + m v_F}, \\ t_1 &= \frac{(E + i\hbar v_F \kappa)}{b} \frac{2\hbar k_3 c (m v_F - \hbar k_3 c^2)}{(\hbar k_3 c^2 + m v_F)^2}, \\ r_\uparrow &= \frac{(E + i\hbar v_F \kappa)}{b} \frac{4\hbar k_3 c^2 m v_F}{(\hbar k_3 c^2 + m v_F)^2}. \end{aligned} \quad (30)$$

Thus, we have shown how to construct a junction of a semi-infinite spinful quantum wire that has four channels (left moving and right moving channels for each of the two spins) with a semi-infinite QSHI edge that has two channels and given formulas for scattering coefficients for electrons incident onto the junction from the quantum wire.

It is interesting to see that for $c = \sqrt{m v_F / \hbar k_3}$, the scattering coefficients in eq. (30) reduce to $r_\downarrow = t_1 = 0$, and $r_\uparrow = (E + i\hbar v_F \kappa)/b$, which means that the electrons incident in the down spin channel get completely reflected into the up spin channel. This happens because of the strong Zeeman field present in region 2 and in region 1 only up spin electrons can transmit. This means that a net spin current flows in region 3 due to a strong Zeeman field applied in region 2.

VII. SUMMARY AND CONCLUSION

To summarize, we studied scattering due to an on-site impurity in one dimension in continuum and lattice models to show that the scattering amplitudes in the two models can be mapped to each other. Then we identified the boundary condition in the continuum theory that captures the problem of scattering due to a bond impurity by introducing a new parameter c . Thus, we have introduced a new boundary condition that describes a tunnel junction in a continuum model wherein the wavefunctions on either sides of the junction may not be equal. It may be noted that the wavefunctions (and their derivative) on either sides of a junction being equal does not conserve current at a junction between the spin orbit coupled region and a metal²⁴. For the particle in a box problem, general boundary conditions wherein a linear combination of the wavefunction and its derivative is set to zero at an end of the box^{25,26} can be employed in place of the typical boundary condition which makes the wavefunction zero at the ends¹. Similarly, the boundary condition introduced in this work for scattering across a point like impurity in a quantum wire is more general.

We also studied the problem of a junction of a quantum wire with infinite edge of QSHI using a boundary condition that uses the parameter c . If the junction between quantum wire and QSHI is described by a lattice model, it is the hopping from quantum wire to the QSHI that is responsible for electron transport from quantum wire to the QSHI edge. This suggests that the parameter c is related to hopping strength between quantum

wire and QSHI. We investigated the dependence of the scattering amplitudes on c and find the value of c for which the transmission across the junction is perfect. A realistic QSHI will have two edges and the parameters c will have two values c_1 and c_2 corresponding to the couplings to the two edges. We perform a systematic study starting from a lattice model for a junction between quantum wire and QSHI and find the parameter c_1 as a function of the hopping amplitude w_{nq} that connects the quantum wire to QSHI. Further, we construct a model in which four channels of spinful quantum wire are connected with two channels of QSHI edge by introducing a Zeeman field over a semi-infinite patch on QSHI edge in the direction perpendicular to the spin easy axis of the edge state electrons. If \hat{z} is the direction of spin of the electrons moving away from the junction in the QSHI edge in such a junction, the incident electrons from quantum wire with spin pointing along $-\hat{z}$ flip their spin into \hat{z} direction completely on reflection and the transmission probability onto the QSHI edge state is zero for a special value of c . This fact could be useful in spintronic applications.

A junction of quantum wire with QSHI edge states that transmits perfectly at all energies is characterized by the boundary condition in eq. (11) with the choice of parameters $\chi_3 = 0$ and $c = \sqrt{mv_F/\hbar k_3}$. This means c needs to be a function of energy. The exact dependence

of c on energy in the generic system needs to be derived from the lattice model of the full system. However, it can be said that c is a smoothly varying function of energy and at some particular energy at which $c = \sqrt{mv_F/\hbar k_3}$, the transmission is perfect.

It has been proposed that edge states of QSHI host exotic Majorana fermions at the interface of a ferromagnet (the region exposed to Zeeman field) and a region that has superconductivity²⁷. Zero bias conductance peak is a feature of Majorana fermions. Such a junction can possibly be probed by an external STM tip for zero bias conductance peak²⁰. The boundary condition discussed in this work can be used to describe the STM tip connected to a ferromagnet-superconductor junction on QSHI edge. In future devices which consist of QSHI and normal metal quantum wires as components, the boundary conditions described in this work can be used to calculate transport properties.

ACKNOWLEDGMENTS

The author thanks Deepak Dhar, Sumathi Rao and Diptiman Sen for stimulating discussions and Ranjan Laha for help with Mathematica. The author also thanks anonymous referee for useful comments. The author thanks DST-INSPIRE Faculty Award (Faculty Reg. No. : IFA17-PH190) for financial support.

* abhirams@uohyd.ac.in

¹ D. J. Griffiths, *Introduction to Quantum Mechanics*, 2nd ed. (Prentice Hall, 2004).

² A. Soori and D. Sen, "Nonadiabatic charge pumping by oscillating potentials in one dimension: Results for infinite system and finite ring," *Phys. Rev. B* **82**, 115432 (2010).

³ A. Agarwal and D. Sen, "Charge transport in a tomonaga-luttinger liquid: Effects of pumping and bias," *Phys. Rev. B* **76**, 035308 (2007).

⁴ G. E. Blonder, M. Tinkham, and T. M. Klapwijk, "Transition from metallic to tunneling regimes in superconducting microconstrictions: Excess current, charge imbalance, and supercurrent conversion," *Phys. Rev. B* **25**, 4515 (1982).

⁵ K. Pasanai, "Similarities of coherent tunneling spectroscopy of ferromagnet/ferromagnet junction within two interface models: Delta potential and finite width model," *J. Magn. Magn. Mater.* **401**, 463 – 471 (2016).

⁶ D. Suri, R. S. Patel, and A. Soori, "Electron transport in magnetic tunnel junctions – a theoretical study of lattice and continuum models," *arXiv: 1708.03161* (2017).

⁷ C. L. Kane and M. P. A. Fisher, "Transmission through barriers and resonant tunneling in an interacting one-dimensional electron gas," *Phys. Rev. B* **46**, 15233–15262 (1992).

⁸ M. Z. Hasan and C. L. Kane, "Colloquium: Topological insulators," *Rev. Mod. Phys.* **82**, 3045–3067 (2010).

⁹ X.-L. Qi and S.-C. Zhang, "Topological insulators and superconductors," *Rev. Mod. Phys.* **83**, 1057–1110 (2011).

¹⁰ K. v. Klitzing, G. Dorda, and M. Pepper, "New method for high-accuracy determination of the fine-structure constant based on quantized Hall resistance," *Phys. Rev. Lett.* **45**, 494–497 (1980).

¹¹ F. D. M. Haldane, "Model for a quantum hall effect without Landau levels: Condensed-matter realization of the "parity anomaly"," *Phys. Rev. Lett.* **61**, 2015–2018 (1988).

¹² C. L. Kane and E. J. Mele, "Quantum spin Hall effect in graphene," *Phys. Rev. Lett.* **95**, 226801 (2005).

¹³ B. A. Bernevig, T. L. Hughes, and S.-C. Zhang, "Quantum spin Hall effect and topological phase transition in HgTe quantum wells," *Science* **314**, 1757–1761 (2006).

¹⁴ M. König, S. Wiedmann, C. Brüne, A. Roth, H. Buhmann, L. W. Molenkamp, X.-L. Qi, and S.-C. Zhang, "Quantum spin hall insulator state in hgte quantum wells," *Science* **318**, 766–770 (2007).

¹⁵ Z.-Y. Jia, Y.-H. Song, X.-B. Li, K. Ran, P. Lu, H.-J. Zheng, X.-Y. Zhu, Z.-Q. Shi, J. Sun, J. Wen, D. Xing, and S.-C. Li, "Direct visualization of a two-dimensional topological insulator in the single-layer 1T' – WTe₂," *Phys. Rev. B* **96**, 041108 (2017).

¹⁶ L. Peng, Y. Yuan, G. Li, X. Yang, J.-J. Xian, C.-J. Yi, Y.-G. Shi, and Y.-S. Fu, "Observation of topological states residing at step edges of WTe₂," *Nature Communications* **8**, 659 (2017).

¹⁷ S. Modak, K. Sengupta, and D. Sen, "Spin injection into a metal from a topological insulator," *Phys. Rev. B* **86**, 205114 (2012).

- ¹⁸ A. Soori, O. Deb, K. Sengupta, and D. Sen, "Transport across a junction of topological insulators and a superconductor," *Phys. Rev. B* **87**, 245435 (2013).
- ¹⁹ D. Suri and A. Soori, "Finite transverse conductance in topological insulators under an applied in-plane magnetic field," *J. Phys. : Condens. Matter* **33**, 335301 (2021).
- ²⁰ B. Lu, G. Cheng, P. Burset, and Y. Tanaka, "Identifying Majorana bound states at quantum spin Hall edges using a metallic probe," *arXiv: 2110.04472* (2021).
- ²¹ D. Sen and O. Deb, "Junction between surfaces of two topological insulators," *Phys. Rev. B* **85**, 245402 (2012); "Erratum: Junction between surfaces of two topological insulators [*Phys. Rev. B* 85, 245402 (2012)]," *Phys. Rev. B* **86**, 039902 (2012).
- ²² S-Q. Shen, *Topological Insulators* (Springer, 2012).
- ²³ A. Soori, S. Das, and S. Rao, "Magnetic-field-induced Fabry-Pérot resonances in helical edge states," *Phys. Rev. B* **86**, 125312 (2012).
- ²⁴ A. Soori, "Finite transverse conductance and anisotropic magnetoconductance under an applied in-plane magnetic field in two-dimensional electron gases with strong spin-orbit coupling," *J. Phys. : Condens. Matter* **33**, 335303 (2021).
- ²⁵ M. Carreau, E. Farhi, and S. Gutmann, "Functional integral for a free particle in a box," *Phys. Rev. D* **42**, 1194–1202 (1990).
- ²⁶ A. Soori and S. Mukerjee, "Enhancement of crossed Andreev reflection in a superconducting ladder connected to normal metal leads," *Phys. Rev. B* **95**, 104517 (2017).
- ²⁷ L. Fu and C. L. Kane, "Josephson current and noise at a superconductor/quantum spin Hall insulator/superconductor junction," *Phys. Rev. B* **79**, 161408 (2009).